Coordinate Regulation of the Mother Centriole Component Nlp by Nek2 and Plk1 Protein Kinases

Joseph Rapley,[1][†][‡] Joanne E. Baxter,[1][†] Joelle Blot,[1] Samantha L. Wattam,[1] Martina Casenghi,[2] Patrick Meraldi,[2][§] Erich A. Nigg,[2] and Andrew M. Fry[1]*

Department of Biochemistry, University of Leicester, Leicester, United Kingdom,[1] and Department of Cell Biology, Max Planck Institute of Biochemistry, Martinsried, Germany[2]

Mitotic entry requires a major reorganization of the microtubule cytoskeleton. Nlp, a centrosomal protein that binds γ-tubulin, is a G_2/M target of the Plk1 protein kinase. Here, we show that human Nlp and its *Xenopus* homologue, X-Nlp, are also phosphorylated by the cell cycle-regulated Nek2 kinase. X-Nlp is a 213-kDa mother centriole-specific protein, implicating it in microtubule anchoring. Although constant in abundance throughout the cell cycle, it is displaced from centrosomes upon mitotic entry. Overexpression of active Nek2 or Plk1 causes premature displacement of Nlp from interphase centrosomes. Active Nek2 is also capable of phosphorylating and displacing a mutant form of Nlp that lacks Plk1 phosphorylation sites. Importantly, kinase-inactive Nek2 interferes with Plk1-induced displacement of Nlp from interphase centrosomes and displacement of endogenous Nlp from mitotic spindle poles, while active Nek2 stimulates Plk1 phosphorylation of Nlp in vitro. Unlike Plk1, Nek2 does not prevent association of Nlp with γ-tubulin. Together, these results provide the first example of a protein involved in microtubule organization that is coordinately regulated at the G_2/M transition by two centrosomal kinases. We also propose that phosphorylation by Nek2 may prime Nlp for phosphorylation by Plk1.

Microtubules have diverse functions during cell cycle progression. In interphase, long, relatively stable microtubules contribute to the determination of cell shape, morphological changes required for cell migration, intracellular transport of proteins, mRNAs, and macromolecular assemblies, and positioning of membrane-bound organelles such as the Golgi complex and endoplasmic reticulum. In mitosis, shorter, more dynamic microtubules are involved in mitotic spindle organization, spindle positioning through cortical attachment, and determination of the cleavage plane via central spindle interactions (5, 36). These quite distinct sets of activities require significant changes to take place in the organization of microtubules at the transition between interphase and mitosis. These are regulated largely by posttranslational modifications of microtubule- and centrosome-associated proteins.

The centrosome is the primary site of microtubule nucleation in animal cells, consisting of two cylindrical centrioles surrounded by a meshwork of fibrous and globular proteins that together constitute the pericentriolar material (1, 8). Within the pericentriolar material, γ-tubulin ring complexes are concentrated through interaction with γ-tubulin binding proteins, including pericentrin, pericentrin B/kendrin, CG-NAP, CP309, and Asp (6, 7, 28, 50). γ-Tubulin ring complexes promote the nucleation of microtubules, probably through act-

ing as structural templates for the minus ends of microtubules (27). Following nucleation, some microtubules are released from the centrosome with γ-tubulin ring complexes still capping the minus ends (29). Alternatively, microtubules may be severed close to their minus ends by proteins such as katanin (23). Released microtubules may migrate to distant locations within the cell or be captured by anchoring proteins that bind to either the plus or minus end of microtubules (1, 47). One microtubule minus-end-anchoring protein is ninein, a large coiled-coil protein with no obvious enzyme activity (39, 45). Ninein is localized at the centrosome in most cells but is also found at noncentrosomal apical sites of microtubule anchoring in specialized cell types such as cochlear epithelial cells (2, 39). At the centrosome, ninein is preferentially concentrated on the distal appendages of the older of the two centrioles, the mother, leading to the hypothesis that these appendages act as sites of microtubule anchoring (44). However, the mechanism by which ninein anchors microtubules is not known.

A protein with substantial sequence similarity to ninein was recently identified as a binding partner of the centrosomal protein kinase Plk1 (Polo-like kinase 1). This protein, termed ninein-like protein (Nlp), is concentrated at the centrosome in interphase cells but barely detectable on mitotic spindle poles (3). Nlp interacts with components of the γ-tubulin ring complex, raising the possibility that it contributes to microtubule nucleation during interphase but not mitosis. When overexpressed, Nlp forms large assemblies surrounding the centrosome that can be dispersed by coexpression of active but not inactive Plk1. As Plk1 itself becomes localized to the centrosome in late G_2 and has peak activity at the G_2/M transition (19), a model was proposed in which Plk1 phosphorylation stimulates removal, by either displacement or degradation, of Nlp from the centrosome. In support of this hypothesis, mu-

* Corresponding author. Mailing address: Department of Biochemistry, University of Leicester, University Rd., Leicester LE1 7RH, United Kingdom. Phone: 44 116 252 5024. Fax: 44 116 252 3369. E-mail: amf5@le.ac.uk.

† J.R. and J.E.B. contributed equally to this work.

‡ Present address: Department of Molecular Biology, Massachusetts General Hospital, Boston, Mass.

§ Present address: Department of Biology, Massachusetts Institute of Technology, Cambridge, Mass.

tation of eight putative Plk1 phosphorylation sites in the N-terminal half of Nlp prevented Plk1 from triggering Nlp removal from the centrosome and consequently led to severe defects in mitotic spindle formation (3).

One mechanism of substrate recognition by Plks has recently been described. Plks contain a highly conserved polo box domain in the noncatalytic C-terminal half of the protein. This domain, which is required for centrosome localization (26, 46, 48, 49), forms a cleft that binds a phosphoserine or phosphothreonine in an S-(pS/pT) motif (4, 10). Thus, efficient recognition of certain substrates by Plks may require prior phosphorylation by a so-called priming kinase. So far, Cdk1 and Plk1 itself have been proposed as priming kinases for substrate recognition by Plk1 (11, 41). However, other kinases active at the G_2/M transition (43) may also function in priming substrates for recognition by Plk1.

One such kinase that is active in late G_2 and localized to the centrosome is Nek2. Nek2 is a member of the NIMA-related kinase family and contributes to centrosome separation at the G_2/M transition (13). During interphase, mother and daughter centrioles are held in close proximity to each other through a specialized portion of pericentriolar material known as the intercentriolar linkage. Following duplication of centrioles, Nek2 triggers dissolution of this linkage, possibly as a result of phosphorylation of a core centriolar component C-Nap1 (16, 34, 35). Expression of kinase-inactive Nek2 interferes with bipolar spindle formation and chromosome segregation, raising the possibility that Nek2 has multiple centrosomal substrates at the G_2/M transition (12).

We were therefore led to ask whether Nlp might also be a Nek2 substrate. In this article, we report that Nlp is a mother centriole-specific protein that is displaced from the centrosome at the G_2/M transition. We also show that Nlp can indeed be phosphorylated by Nek2 both in vitro and in vivo. Overexpression of Nek2 and of Plk1 has similar consequences in that it can displace Nlp from interphase centrosomes as well as fragment recombinant Nlp assemblies. However, phosphorylation of Nlp by Nek2 occurs on sites that are distinct from those phosphorylated by Plk1, and kinase-inactive Nek2 can interfere with phosphorylation of Nlp by Plk1. These results highlight the complex mechanisms of phosphorylation that are employed to ensure proper regulation of microtubule organization during mitotic onset and raise the possibility that Nek2 is a priming kinase for Plk1.

MATERIALS AND METHODS

Cell culture, synchronization, and transfection. *Xenopus laevis* A6 adult kidney and XTC cells were grown at 23°C in modified (60% medium, 40% water) Leibovitz L15 medium (Invitrogen, Paisley, United Kingdom) supplemented with 10% heat-inactivated fetal calf serum (Invitrogen) and penicillin-streptomycin (100 IU/ml and 100 mg/ml, respectively). The U2OS osteosarcoma cell line expressing Nek2A-K37R-Myc-His from a tetracycline-inducible cytomegalovirus promoter has been described (12). These, together with standard U2OS cells, were grown in Dulbecco's modified Eagle's medium (Invitrogen) supplemented with 10% heat-inactivated fetal calf serum, 100 IU of penicillin per ml, and 100 mg of streptomycin per ml at 37°C in a 5% CO_2 atmosphere. To induce and maintain expression from tetracycline-responsive promoters, tetracycline or doxycycline (1 μg/ml) was added to the culture medium every 24 h (12).

For synchronization, A6 cells were grown to approximately 50% confluency and then treated accordingly. For G_0, cells were transferred to serum-free medium for 48 h. For G_1/S, hydroxyurea was added to a 1 mM final concentration for 24 h. For S/G_2 and G_1 populations, a G_1/S block was imposed, followed by

replacement with drug-free medium for 8 and 16 h, respectively. A mitotic population was generated by addition of nocodazole to a final concentration of 500 ng/ml for 24 h. The percentage of cells in each phase of the cell cycle was calculated by standard flow cytometry following propidium iodide staining. For transient transfections, A6 or U2OS cells were grown to approximately 50% confluency and transfected with Lipofectamine 2000 according to the manufacturer's instructions (Invitrogen). Unless otherwise indicated, transfected cells were incubated for 24 h prior to fixation for immunofluorescence microscopy or cell extraction.

Plasmid constructions. Expressed sequence tags (ESTs) containing overlapping *Xenopus laevis* Nlp (X-Nlp) sequences were obtained from the National Institute for Basic Biology, Okazaki, Japan (XL076, XL082, and XL088) and MRC Geneservice, Cambridge, United Kingdom (image clone 6630669). A short X-Nlp cDNA lacking the 439-amino-acid insertion was first generated by introducing a SalI restriction site into XL082 and XL076 with the GeneTailor site-Directed mutagenesis kit (Invitrogen). An EcoRI-SalI fragment was then excised from XL082 and subcloned into the EcoRI and SalI sites of XL076. The SalI site was then mutated back to the original sequence, creating pBS:X-Nlp-ΔN, which lacks the N-terminal 260 amino acids. A 951-bp EcoRI fragment from image clone 6630669 containing the N-terminal sequence was then subcloned into the EcoRI sites of the newly generated pBS:X-Nlp-ΔN construct, giving pBS:X-Nlp-short. To generate the complete full-length X-Nlp cDNA encoding a protein of 1,836 amino acids, overlapping PCRs were performed on image clone 6630669 with primers SW013 (GCGCTCTAGAATGGACAAGGAAGAAGAGAAT) and SW014 (AATGTTCCACCTCCTTCC) and pBS:X-Nlp-short with primers SW015 (ATGGAGCTCTGCCGTCTG) and SW016 (GCGCAAGCTTTCA-GACTGCAAGAGAGGC).

The two PCR products were mixed and a further PCR was performed with primers SW013 and SW016. The product was subcloned into pGEM-Teasy (Promega, Southampton, United Kingdom) to generate pGEM:X-Nlp-FL. Fragments encoding amino acid residues 262 to 552 and 1239 to 1836 were subcloned into the pET32-C1 vector (containing an N-terminal Trx-His-S tag; Merck Biosciences, Nottingham, United Kingdom) to generate pET32:X-Nlp$_{262-552}$ and pET32:X-Nlp$_{1239-1836}$, respectively. The fragment encoding amino acids 262 to 552 was also subcloned into the pMAL-c2G vector (containing an N-terminal maltose-binding protein [MBP] tag; New England Biolabs UK Ltd., Hitchin, United Kingdom) to generate pMAL:X-Nlp$_{262-552}$. Yeast two-hybrid constructs were generated by inserting the full-length X-Nek2A-K37R cDNA into the Gal4 DNA binding domain vector pGBDU (25), creating pGBDU:X-Nek2A-K37R. The X-Nlp fragment in the Gal4 activation domain vector pACT2 (BD Biosciences, Oxford, United Kingdom) has been described (3). New constructs were sequenced by Lark Technologies, Inc. (Saffron Walden, United Kingdom). All other Nek2 (15, 17), Nlp (3), Plk1 (37), and Aurora A (37) constructs used here have been described previously.

Bacterial expression and protein purification. The pET32-X-Nlp constructs were expressed in *Escherichia coli* Rosetta DE3 (Merck Biosciences) following induction at 37°C with 1 mM isopropylthiogalactopyranoside (IPTG) and purified with the His tag under denaturing conditions by Ni^{2+}-agarose affinity chromatography according to the manufacturer's instructions (Qiagen Ltd., Crawley, United Kingdom). The pMAL-X-Nlp$_{262-552}$ construct was expressed in *E. coli* Rosetta DE3 following induction at 37°C with 0.4 mM IPTG and purified by amylose resin chromatography according to the manufacturer's instructions (New England Biolabs UK Ltd.).

Antibody generation. Antibody production was carried out by Cambridge Research Biochemicals (Cleveland, United Kingdom). Rabbits were first screened to eliminate those with centrosome-reactive sera before five (R688) or seven (R1679) injections of selected rabbits with 0.5 mg of Trx-S-His-X-Nlp fusion protein according to standard immunization protocols. Rabbit bleeds were screened by Western blotting of A6 cell lysates and immunofluorescence microscopy of methanol-fixed A6 cells. For affinity purification of R1679 antiserum, an MBP-X-Nlp$_{262-552}$ Affigel column was made according to the manufacturer's instructions (Bio-Rad, Hemel Hempstead, United Kingdom). After extensive column washes with 10 mM Tris-HCl (pH 7.5) followed by 10 mM Tris-HCl (pH 7.5)–500 mM NaCl, specific antibodies were eluted with 100 mM glycine (pH 2.5) into tubes containing neutralizing quantities of 1 M Tris-HCl (pH 8.0). For competition with antigen, 375 ng of affinity-purified antibody was incubated with 2 μg of MBP-X-Nlp$_{262-552}$ prior to immunofluorescence staining of A6 cells.

Preparation of extracts, protein electrophoresis, and Western blotting. Extracts of cultured human and *Xenopus* cells were prepared in NP-40 lysis buffer (150 mM NaCl, 1% NP-40, 50 mM Tris-HCl, pH 8). Low-speed cytoplasmic extracts of metaphase II (cytostatic factor [CSF])-arrested eggs or eggs induced to enter interphase by addition of calcium ionophore were prepared as described previously (22). Sodium dodecyl sulfate (SDS)-polyacrylamide gel electrophore-

sis and Western blotting were performed as previously described (16). For Western blotting of X-Nlp, 5% polyacrylamide gels were used; otherwise, all gels were 12% polyacrylamide. Primary antibodies used were anti-X-cyclin B2 (2 μg/ml; gift from H. Yamano, South Mimms, United Kingdom), anti-Eg2 (1:500), anti-green fluorescent protein (anti-GFP) (0.1 μg/ml; Abcam, Cambridge, United Kingdom), anti-Myc (1:1,000; Cell Signaling Technologies, Beverly, Mass.), anti-X-Nlp (2.5 μg/ml for purified R1679; 1:500 for R668), anti-Nek2 (1 μg/ml; Zymed) (14), and anti-α-tubulin (1:2,000; Sigma, Poole, United Kingdom), while secondary antibodies were alkaline phosphatase-conjugated anti-rabbit or anti-mouse immunoglobulin G (1:7,500; Promega).

Immunofluorescence microscopy. Immunofluorescence microscopy was performed as previously described (12). Cells were fixed with either methanol (−20°C) for 6 min or paraformaldehyde solution (3% paraformaldehyde, 2% sucrose, 1× phosphate-buffered saline) for 10 min at room temperature. Paraformaldehyde-fixed cells were permeabilized by 5 min of incubation in 0.5% Triton X-100 (in 1× phosphate-buffered saline). Primary antibodies used were raised against human Nek2 (1 μg/ml Zymed polyclonal [14] or 1 μg/ml Transduction Laboratories monoclonal), *Xenopus* Nek2 (2 μg/ml; R81) (15), human Nlp (1 μg/ml (3), *Xenopus* Nlp (2.5 μg/ml), γ-tubulin (0.15 μg/ml; Sigma), C-Nap1 (1 μg/ml; R63) (16), Myc (1:2,000; Cell Signaling Technologies), or polyglutamylated tubulin (GT335; 0.3 μg/ml; gift from B. Edde, Montpellier, United Kingdom). Secondary antibodies used were Alexa Fluor 488 or 594 goat anti-rabbit and anti-mouse immunoglobulin G (1 μg/ml; Invitrogen), donkey anti-rabbit and sheep anti-mouse biotinylated whole antibodies (1:100; Amersham Biosciences, Little Chalfont, United Kingdom). Streptavidin-Texas Red (1:200; Amersham Biosciences) was used to detect biotinylated antibodies, while DNA was stained with Hoechst 33258 (0.2 μg/ml; Calbiochem, San Diego, Calif.).

Fluorescence images were captured on a TE300 inverted microscope (Nikon United Kingdom, Ltd., Kingston upon Thames, United Kingdom) with an Orca ER charge-coupled device camera (Hamamatsu, Hamamatsu, Japan) with Openlab 3.14 software (Improvision, Coventry, United Kingdom) and processed with Adobe Photoshop (San Jose, Calif.). Quantitative imaging was performed by measuring the mean pixel intensity at nonsaturating exposure conditions with Openlab 3.14 software (Improvision) within a fixed region of interest (1 μm²). Background readings were taken on neighboring regions of the cell and subtracted from the centrosome intensity measurements.

Miscellaneous techniques. Yeast two-hybrid analysis was performed with the PJ694A strain as previously described (25). *lacZ* reporter gene expression was assayed with the β-galactosidase substrate *O*-nitrophenyl-β-D-galactopyranoside, as described (9). In vitro kinase assays were performed with wild-type or kinase-inactive human Plk1 (31), human Nek2 (18), or *Xenopus* Nek2 (51) kinases purified from insect cells following infection with recombinant baculoviruses or Myc-tagged Nek2 kinases immunoprecipitated with anti-Myc antibodies (Cell Signaling Technologies) from transfected U2OS cells as described (18). X-Nlp was translated in vitro from pGEM:X-Nlp-FL with a T7 polymerase in conjunction with the TnT-coupled transcription-translation kit according to the manufacturer's instructions (Promega). Destruction assays in *Xenopus* egg extracts were performed as previously described (22). Microtubule regrowth assays were performed as described previously (38).

Nucleotide sequence accession number. The GenBank accession number for X-Nlp is AY566230.

RESULTS

***Xenopus laevis* Nlp is a centrosomal protein.** Nlp was first identified in a yeast two-hybrid interaction screen of a *Xenopus* oocyte cDNA library with the kinase-inactive version of *Xenopus* Plx1 (N172A) as the bait. The cDNA fragment isolated matched a full-length human cDNA (KIAA0980), and hence, the human clone was used to characterize the properties and regulation of Nlp (3). To extend these studies, we have now obtained overlapping EST sequences from *Xenopus laevis* that encode an X-Nlp protein of 1,836 amino acids with a predicted molecular mass of 213 kDa. This is somewhat larger than the published human Nlp sequence (156 kDa) but close to the predicted size of a rat Nlp homologue present in the database. We note that one *Xenopus* EST lacked an internal sequence encoding 439 amino acids after residue 792 that would lead to

a putative protein of 162 kDa. Thus, it is possible that vertebrates express at least two splice variants of Nlp.

X-Nlp protein shares 60% similarity with human Nlp in the N-terminal half of the protein (amino acids 1 to 691) and 86% similarity over the C-terminal 80 amino acids (Fig. 1A). Between these two regions there is little sequence similarity, but both proteins are predicted to form extended coiled coils (33). Like human Nlp and ninein, X-Nlp also has two putative Ca^{2+}-binding EF-hand motifs within its N terminus. Antibodies were raised in rabbits with bacterially expressed His-tagged fusions of two distinct regions of X-Nlp (R1679 to amino acids 262 to 552 and R688 to amino acids 1239 to 1836). R1679 was affinity purified with a bacterially expressed fusion of amino acids 262 to 552 to MBP. On Western blots of *Xenopus* A6 adult kidney cell extracts, both antibodies (plus four other rabbit immune antisera not described) recognized a common band at 210 kDa, the predicted size of X-Nlp (Fig. 1B).

Translation of X-Nlp in vitro generated a product that was recognized by the affinity-purified R1679 antibody and that comigrated with the band detected in A6 cells (Fig. 1C). By immunofluorescence microscopy, both antibodies stained centrosomes in methanol (Fig. 1D and E) and paraformaldehyde (data not shown) fixed A6 cells as indicated by colocalization with γ-tubulin. Centrosome staining and reactivity of the 210-kDa protein on Western blots with the affinity-purified R1679 was completely blocked by preincubation with the MBP:X-Nlp$_{262-552}$ protein (Fig. 1D and data not shown). Depolymerization of microtubules by incubating A6 cells on ice in the presence of 6 μg of nocodazole per ml had no effect on the centrosome staining pattern (data not shown). X-Nlp is therefore a bona fide core centrosomal protein in adult *Xenopus* cells.

Nlp is displaced from spindle poles but not degraded in mitosis. Immunofluorescence microscopy of *Xenopus* A6 cells at different stages of the cell cycle revealed that X-Nlp is strongly associated with interphase centrosomes, but much less prominent on mitotic spindle poles (Fig. 2A). Quantitative imaging revealed that X-Nlp began to disappear from centrosomes in prophase and by metaphase had decreased to <20% of the abundance during interphase (Fig. 2B). This reduced level of X-Nlp was maintained in anaphase and telophase cells, with X-Nlp only reaccumulating at the centrosome following cytokinesis. Identical results were obtained in two cell lines (A6 and XTC) with both antibodies, making the possibility of epitope masking highly unlikely.

These findings fall in line with studies in human cells, although it is worth noting that, in prophase, Nlp is virtually undetectable in human U2OS cells (3) (see Fig. 6A) but is only beginning to diminish in *Xenopus* A6 cells (Fig. 2B). Previous work did not distinguish whether the reduction in Nlp intensity was due to displacement from the centrosome or degradation. We therefore performed Western blots on extracts of A6 cells synchronized at different stages of the cell cycle (Fig. 2C). Synchrony was confirmed by Western blotting for cyclin B2 and the *Xenopus* Aurora A protein Eg2 (Fig. 2C) and by flow cytometry (data not shown).

The total abundance of X-Nlp was unchanged throughout the cell cycle and clearly was not reduced in mitotic cells. Furthermore, destruction assays confirmed that in vitro-translated X-Nlp was stable in mitotic extracts of *Xenopus* eggs
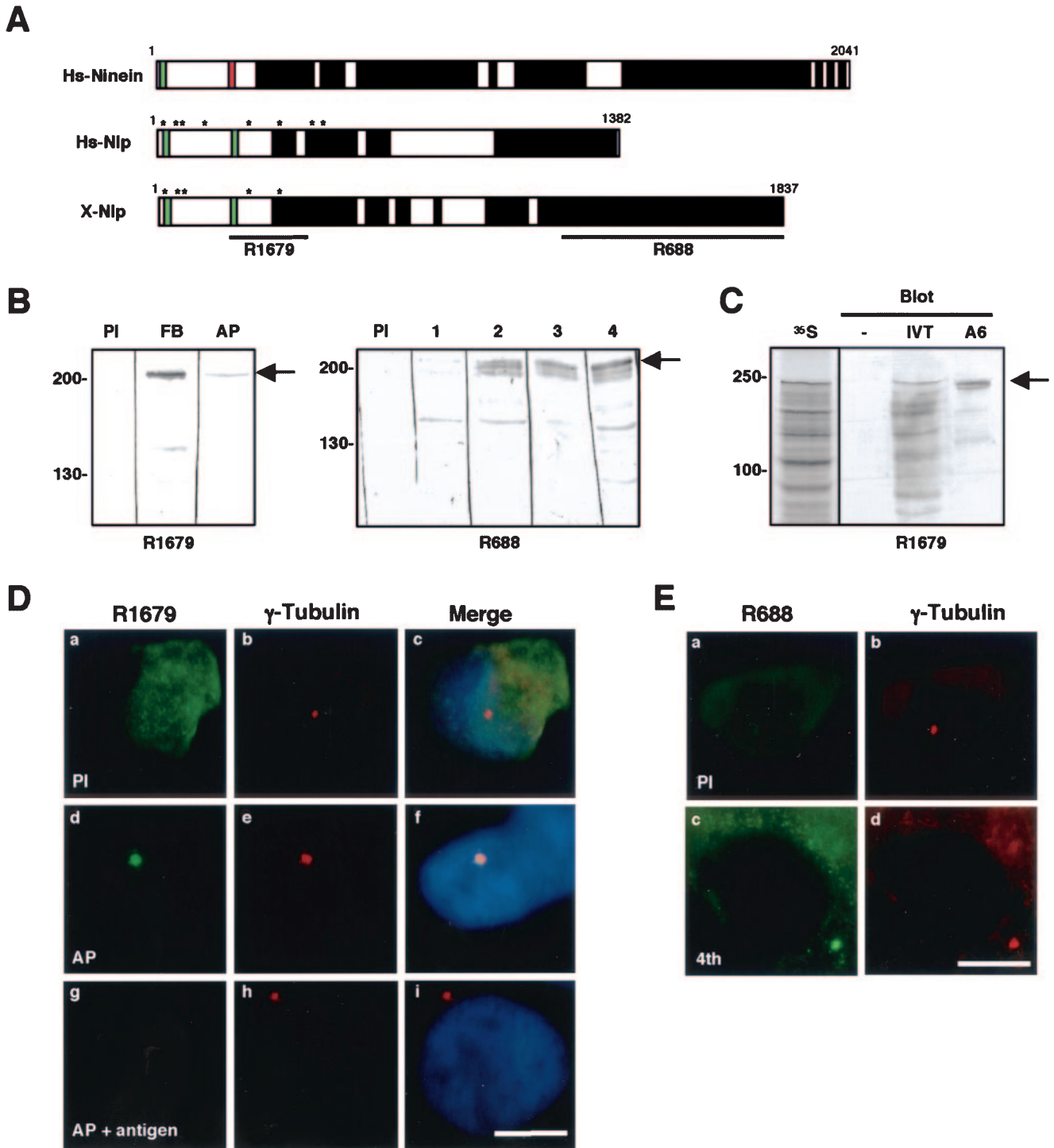
FIG. 1. X-Nlp is a *Xenopus laevis* centrosomal protein. (A) Schematic comparison of human ninein (Hs-Ninein), human Nlp (Hs-Nlp), and *Xenopus laevis* Nlp (X-Nlp) proteins. Numbers represent amino acids; putative Ca^{2+}-binding EF-hands (green boxes), GTP-binding site (red box), and coiled coils (black boxes) are indicated. Asterisks represent eight putative Plk1 phosphorylation sites identified in human Nlp (3), of which five are conserved in X-Nlp. The regions of the X-Nlp protein used to generate antisera R1679 and R688 are also indicated. (B) Western blots of *Xenopus* A6 whole-cell extracts with anti-X-Nlp antibodies R1679 (left panel; PI, preimmune serum; FB, final bleed serum; AP, affinity-purified antibodies) and R688 (right panel; PI, preimmune serum; 1 to 4, crude serum from bleeds 1 to 4). (C) Full-length X-Nlp was translated in vitro in the presence of [^{35}S]methionine and, following SDS-PAGE, was either exposed to autoradiography (^{35}S) or Western blotted with affinity-purified R1679 (IVT). In vitro-translated samples lacking input DNA (−) or A6 whole-cell extracts (A6) were Western blotted in parallel. In panels B and C, the positions of molecular size markers are indicated on the left (in kilodaltons), and the X-Nlp protein is indicated by an arrow on the right. (D) Immunofluorescence microscopy of methanol-fixed *Xenopus* A6 cells costained with preimmune (a) or affinity-purified (d and g) R1679 anti-X-Nlp (green) and anti-γ-tubulin (b, e, and h; red) antibodies. Merged images including DNA stain (blue) are also shown (c, f, and i). In panels g to i, affinity-purified anti-X-Nlp antibodies were incubated with an excess of MBP-X-Nlp$_{262–552}$ protein. (E) Immunofluorescence microscopy of methanol-fixed A6 cells costained with preimmune (a) or immune (c; fourth bleed) R688 anti-X-Nlp and anti-γ-tubulin (b and d) antibodies. Scale bars in panels D and E, 10 μm.
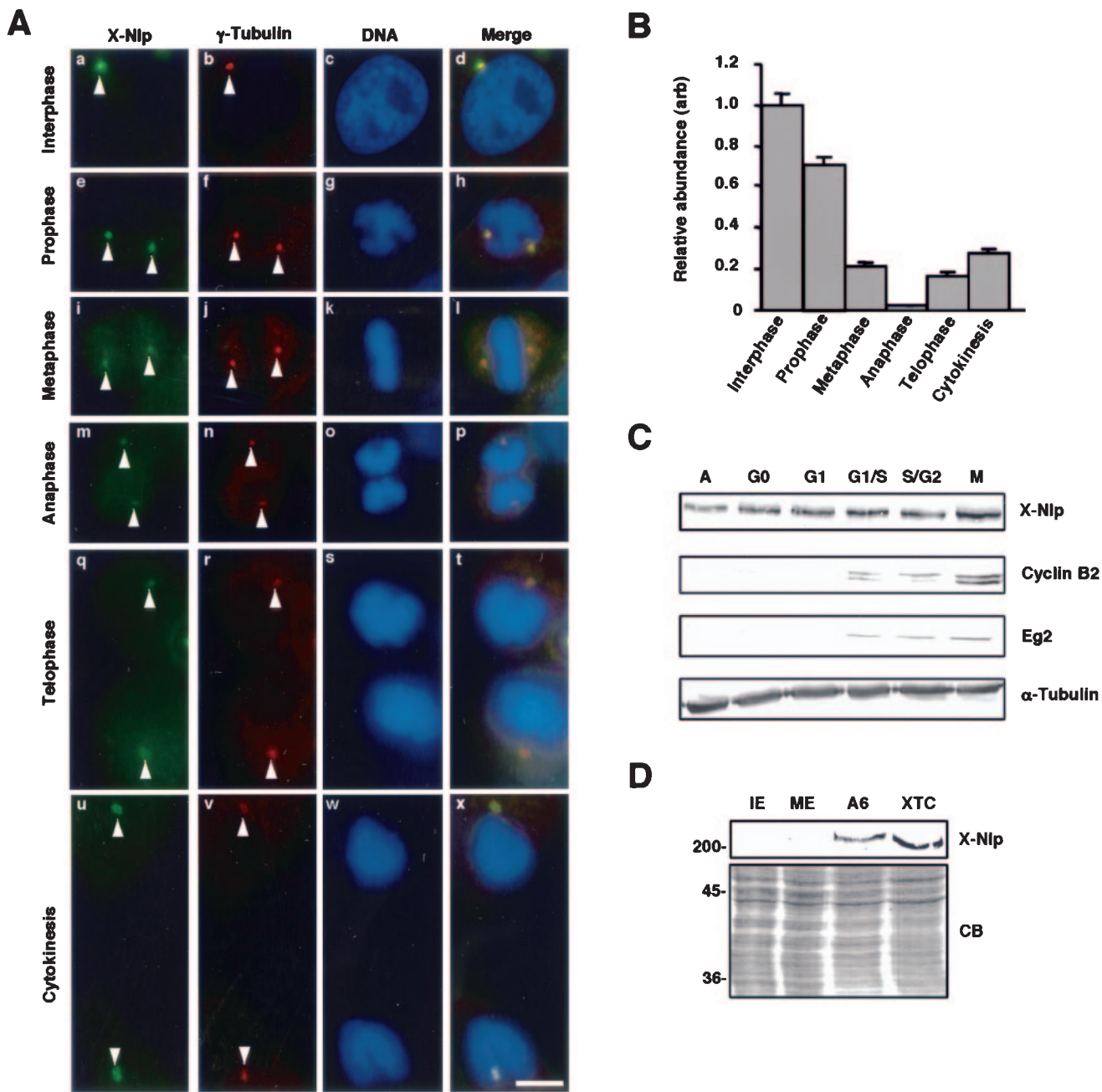
FIG. 2. Localization of X-Nlp at the centrosome is cell cycle dependent. (A) Immunofluorescence microscopy of methanol-fixed *Xenopus* A6 cells at different stages of the cell cycle, as indicated, costained with purified R1679 anti-X-Nlp (green) and anti-γ-tubulin (red) antibodies. DNA was stained with Hoechst 33258 (blue), and merged images are shown. Arrowheads indicate positions of centrosomes/spindle poles. (B) The abundance of X-Nlp at a pair of interphase centrosomes (given an arbitrary value of 1.0) was compared with that at the two spindle poles (added together) in different stages of mitosis by quantitative fluorescence imaging as described in Materials and Methods. The centrosomes/spindle poles in 20 cells were analyzed for each bar of the histogram, and error bars represent standard deviations. (C) *Xenopus* A6 cells were synchronized in different stages of the cell cycle, as indicated (A, asynchronous), with the procedures described in Materials and Methods. Cell extracts were separated by SDS-PAGE and Western blotted for X-Nlp (purified R1679 antibodies), cyclin B2, Eg2, and α-tubulin. (D) Interphase (IE), and metaphase II (ME)-arrested *Xenopus* egg extracts as well as extracts of A6 and XTC cells were Western blotted for X-Nlp protein (purified 1679 antibodies, upper panel). Equal protein loading was confirmed by Coomassie blue (CB) staining of an equivalent SDS-polyacrylamide gel (lower panel). The positions of molecular size markers are indicated on the left (in kilodaltons).

(data not shown). Hence, the disappearance of Nlp from the spindle poles is best explained by a change in localization and not degradation. Surprisingly, X-Nlp was not detected on Western blots of cytoplasmic extracts prepared from CSF-

arrested eggs or eggs induced to enter interphase by calcium addition (Fig. 2D). Nor could X-Nlp be detected by immunofluorescence microscopy on the centrosome of demembranated sperm either before or after incubation in egg ex-

tracts (data not shown). These data reveal that X-Nlp protein is not expressed in gametes and does not appear on the zygotic centrosome generated in vitro. This implies that centrosomes in early frog embryos are unlikely to require Nlp for organization of interphase microtubules.

Nlp is a mother centriole-specific protein. The hypothesis that ninein contributes to microtubule anchoring is based in large part on its preferential localization to the mother centriole (44). Hence, we examined the distribution of Nlp at centrosomes in interphase A6 cells with purified X-Nlp antibodies. In this cell type, centrosomes as stained with γ-tubulin often appear as a single large spot that is clearly recognized by Nlp antibodies (see Fig. 1D and E). However, in some cells, two γ-tubulin-staining spots can be distinguished, and in this case X-Nlp is restricted to one of the two spots (Fig. 3A).

To determine whether this spot contained the mother or daughter centriole, A6 cells were serum starved, inducing production of primary cilia that could be detected with antibodies against polyglutamylated tubulin (GT335). Antibody costaining demonstrated that X-Nlp is present specifically on the centriole subtending the cilium, i.e., the mother centriole (Fig. 3B). Overexpression of full-length human GFP-Nlp induces the formation of large assemblies that encompass the centrosome (3). Costaining with the centriolar marker C-Nap1 revealed that the two centrioles were frequently separated by >2 μm (Fig. 3C) and, while sometimes both centrioles remained within the large GFP-Nlp assembly, often the bulk of GFP-Nlp was clustered around just one centriole (Fig. 3D). The other centriole was completely devoid of GFP-Nlp, consistent with Nlp protein's only being capable of associating with one centriole. A review of the staining pattern produced by human Nlp antibodies confirmed the presence of three small dots surrounding one centriole and one weaker dot colocalizing with the second centriole (data not shown) (3). This staining pattern is identical to that reported for ninein (39) and provides further support to the notion that ninein and Nlp are both preferentially localized to mother centrioles.

Displacement of endogenous Nlp from the centrosome by active Nek2 kinase. To test the hypothesis that Nlp might be regulated by the Nek2 kinase in addition to Plk1, we first asked whether Nek2 and Nlp can interact in the yeast two-hybrid assay. Vertebrate Nek2 is expressed as two splice variants, Nek2A and Nek2B, which differ in their extreme C termini (21, 52). In embryonic systems, only Nek2B is expressed, whereas in adult cells, Nek2A is the predominant isoform. When cotransformed in *Saccharomyces cerevisiae*, X-Nlp and a kinase-inactive mutant of X-Nek2A (K37R) activated reporter genes to a similar extent as the positive control pairing of SNF1 and SNF4, whereas when transformed with control plasmids, little or no activation of reporters was detected (Fig. 4A).

We next tested whether Nek2A kinase was capable of influencing the distribution of X-Nlp in vivo. For this purpose, A6 cells were transfected with wild-type Nek2A or kinase-inactive Nek2A-K37R and stained for endogenous X-Nlp (Fig. 4B). Wild-type Nek2A led to loss of X-Nlp at the centrosome in 85% of interphase cells, whereas kinase-inactive Nek2A triggered loss in only 22% cells (Fig. 4C). In human U2OS cells, wild-type Nek2A induced a comparable displacement of Nlp from the centrosome in >80% of cells (Fig. 4D), whereas wild-type and kinase-inactive enhanced green fluorescent protein (EGFP)-Aurora A induced Nlp displacement in <10% of cells (Fig. 4E).

The efficient displacement of endogenous Nlp from the interphase centrosome by active Nek2A was highly reminiscent of that seen following transfection of a hyperactive Plk1 (T210D) construct (3). We therefore decided to test whether the kinase-inactive (K/R) mutants could act in a dominant-negative manner to prevent the displacement of Nlp from the centrosome caused by the active enzymes. After 24 h, transfection of either wild-type Nek2A or hyperactive Plk1 alone or the two active kinases together led to loss of Nlp from the centrosome in >80% of U2OS cells, as expected, while the kinase-inactive mutants led to between 25 and 35% loss when transfected alone (Fig. 5A). Intriguingly, when transfected in combination, Plk1-K/R did not prevent wild-type Nek2A from stimulating Nlp displacement, but Nek2A-K/R substantially reduced the ability of hyperactive Plk1 to induce Nlp displacement. The moderate loss of Nlp in the presence of overexpressed inactive kinases may result from either disruption of centrosome structure (17) or steric interference with Nlp association with the centrosome. By analyzing cells after only 16 h of transfection, we found that Nek2A-K/R alone had a less pronounced effect on Nlp localization but that its ability to suppress Nlp displacement by hyperactive Plk1 was undiminished (Fig. 5B and C).

Dominant-negative Nek2A interferes with Nlp displacement from spindle poles. We next tested whether kinase-inactive Nek2A could interfere with displacement of endogenous Nlp from the centrosome during mitosis. For this experiment, we made use of U2OS cells, which express Nek2A-K/R from a tetracycline-inducible promoter (12). In the absence of Nek2A-K/R induction, Nlp abundance was severely diminished at mitotic spindle poles as expected. However, following 24 h of induction, Nlp was much more readily detected on spindle poles during both prophase and metaphase (Fig. 6A and B). Interphase cells expressing kinase-dead Nek2A did not have increased levels of Nlp at the centrosome (data not shown). Hence, kinase-inactive Nek2A acts in a dominant-negative manner to inhibit displacement of Nlp from the mitotic spindle poles.

Nek2A and Plk1 phosphorylation sites are distinct. As shown earlier (Fig. 3D), recombinant GFP-Nlp forms large assemblies, presumably through oligomerization, that surround the mother centriole. Coexpression with wild-type Nek2A but not the kinase-inactive mutant caused the dramatic fragmentation of this large assembly into smaller particles that were distributed throughout the cytoplasm (Fig. 7A). Importantly, the overexpressed Nek2A protein strongly colocalized with Nlp irrespective of whether it was active, supporting the notion that these proteins are capable of interaction in vivo (Fig. 7A). Plk1 is also capable of fragmenting GFP-Nlp assemblies in a kinase-dependent manner (3).

One reason why both Plk1 and Nek2 can disrupt GFP-Nlp oligomerization may be that they target the same critical phosphorylation site(s). A consensus motif for phosphorylation by Plk1 (E/DxS/T) has been proposed (31), whereas the amino acid requirements for phosphorylation by Nek2 are less clear. By scanning the human Nlp sequence, eight putative Plk1 phosphorylation sites have been identified in the N-terminal half of Nlp, and four of these sites (S87 or S88, T161, and S686)
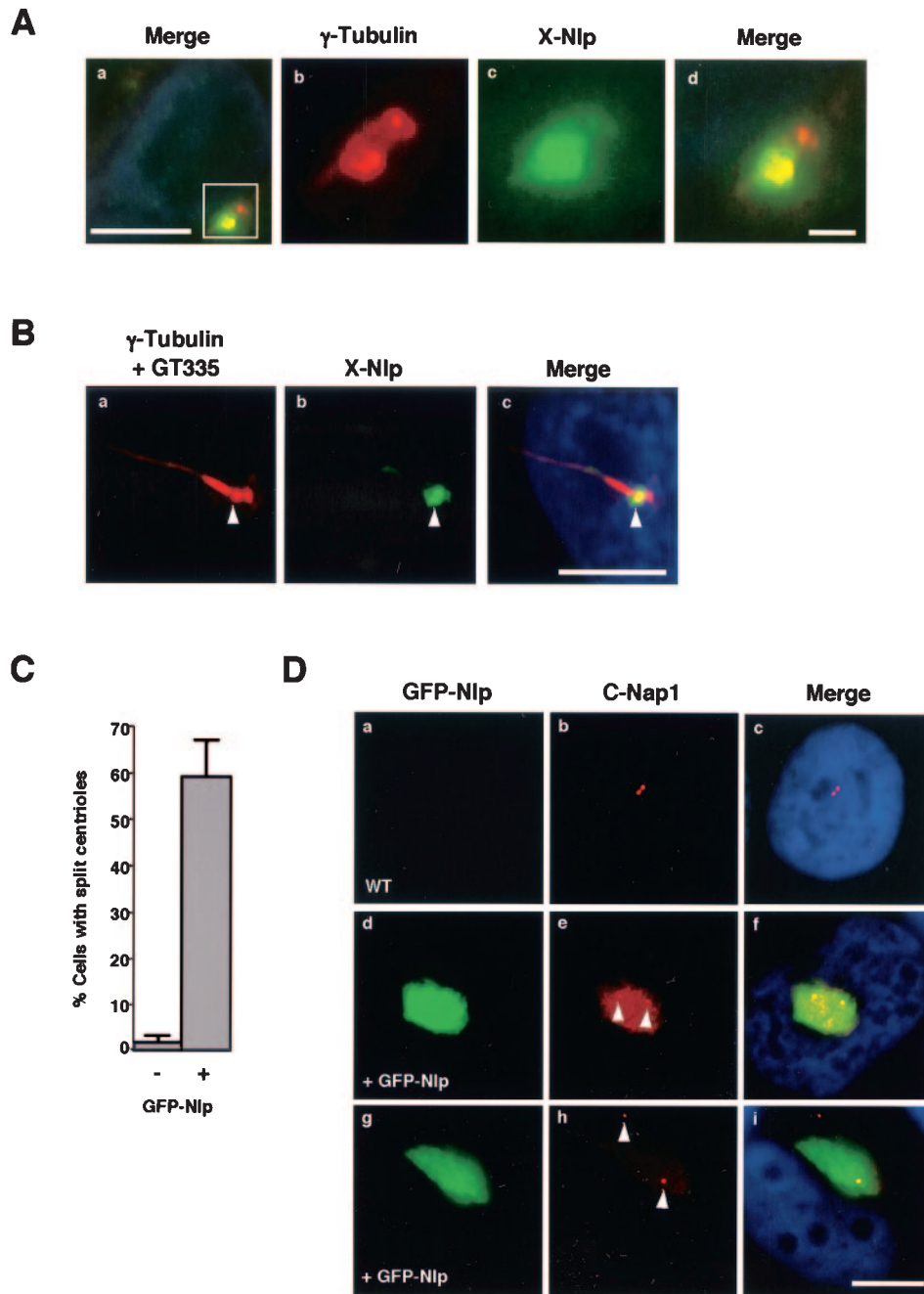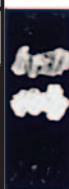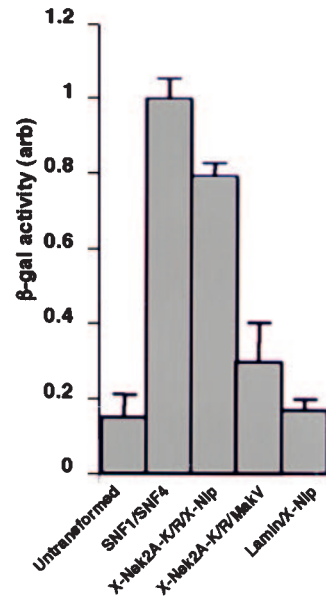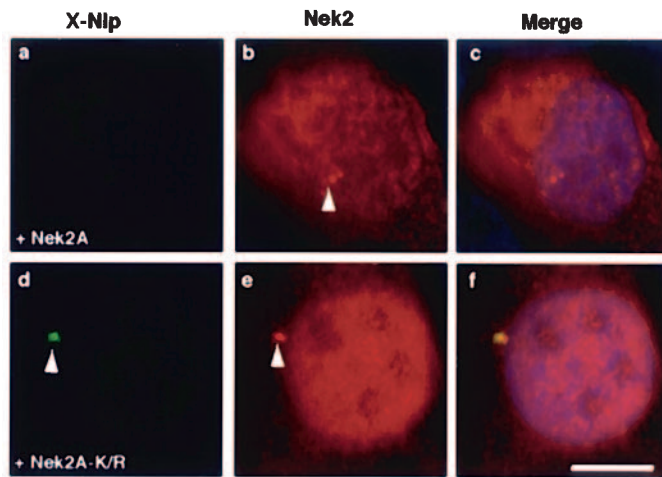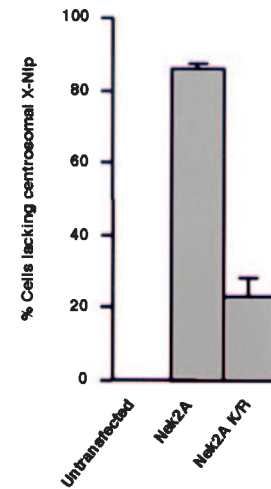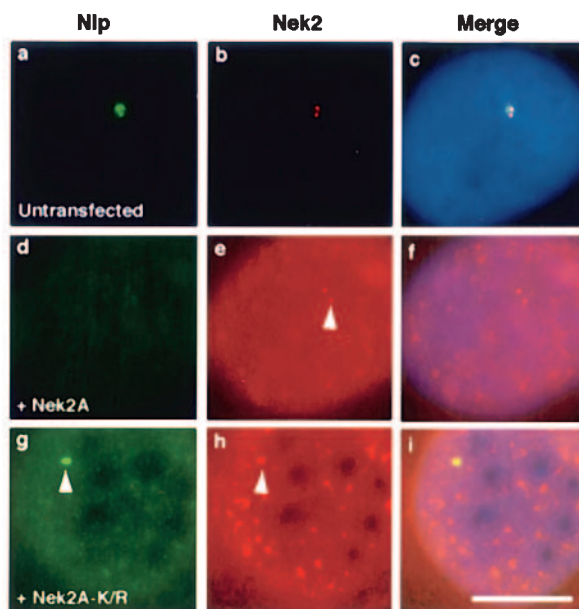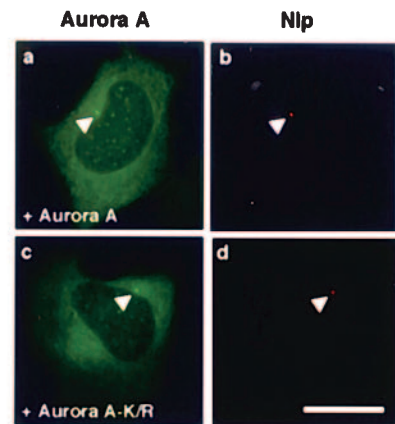
FIG. 3. X-Nlp localizes to the mother centriole in interphase cells. (A) Methanol-fixed *Xenopus* A6 cells were processed for immunofluorescence microscopy with anti-X-Nlp (R1679; green) and anti-γ-tubulin (red) antibodies; DNA was stained with Hoechst 33258 (blue). A merged image of an interphase cell is shown, demonstrating that X-Nlp is only present on one centriole (a). Higher magnification of the boxed area in panel a is shown in panels b (γ-tubulin), c (X-Nlp), and d (merge). Scale bar in panel a, 10 μm; in panel d, 1 μm. (B) *Xenopus* A6 cells were induced to grow primary cilia by serum starvation before processing for immunofluorescence microscopy as in A, except that anti-polyglutamylated tubulin antibodies (GT335) were also added. The red signal (a) is therefore a combination of γ-tubulin (revealing the two centrioles) and polyglutamylated tubulin (revealing the primary cilium). The primary cilium is nucleated from the distal end of the mother centriole (arrowhead), and X-Nlp clearly colocalizes with the mother, and not daughter, centriole. Scale bar, 10 μm. (C) The percentage of cells with centrioles separated by >2 μm was determined in untransfected (−) and GFP-Nlp transfected (+) cells; 100 cells were counted for each sample in three independent experiments. (D) U2OS cells were transfected with GFP-Nlp (green) for 24 h before methanol fixation and processing for immunofluorescence microscopy with antibodies against human C-Nap1 (R63; red). Merged images including DNA stained with Hoechst 33258 (blue) are shown. Centrioles, as indicated by C-Nap1 staining, are often split and, in some cases (d to f), both centrioles are still within the GFP-Nlp assembly, whereas in others (g to i), only one centriole remains within the assembly. Scale bar, 10 μm.

A

DBD	AD
-	-
SNF1	SNF4
X-Nek2A-K37R	X-Nlp
X-Nek2A-K37R	MakV
Lamin A	X-Nlp

B

X-Nlp | Nek2 | Merge

a | b | c
+ Nek2A

d | e | f
+ Nek2A-K/R

C

D

Nlp | Nek2 | Merge

a | b | c
Untransfected

d | e | f
+ Nek2A

g | h | i
+ Nek2A-K/R

E

Aurora A | Nlp

a | b
+ Aurora A

c | d
+ Aurora A-K/R

were shown to be phosphorylated by Plk1 in vitro by mass spectrometry (3). Of these, S87, S88, and S686 are conserved between the human and *Xenopus* Nlp proteins (Fig. 1A). Centrosomal assemblies formed by overexpressing a GFP-Nlp mutant lacking all eight phosphorylation sites (NlpΔ8) were no longer fragmented by Plk1 (3). In contrast, active but not inactive Nek2A could still trigger fragmentation of the large NlpΔ8 assemblies around the centrosome (Fig. 7B). Western blotting of these cell extracts revealed a distinct gel mobility shift of both wild-type Nlp and NlpΔ8 in the presence of wild-type but not inactive Nek2A (Fig. 7C). In combination, Nek2A and Plk1 caused an even greater electrophoretic mobility shift, while kinase-inactive Nek2A blocked the electrophoretic shift induced by hyperactive Plk1 (Fig. 7D) and reduced the ability of Plk1 to induce fragmentation of Nlp assemblies (Fig. 7B). These data indicate that Plk1 and Nek2A do not phosphorylate the same sites within the Nlp protein but that kinase-dead Nek2A can interfere with Plk1 phosphorylation and regulation of Nlp.

Nek2 phosphorylation does not prevent interaction of Nlp with γ-tubulin. Immunostaining cells cotransfected with GFP-Nlp and Nek2A with the GT335 antibody revealed that the Nlp fragments were no longer associated with centrioles (Fig. 8A). Indeed, centrioles were often widely separated, consistent with observations that active Nek2A kinase stimulates centriole splitting (12, 17). Thus, Nek2A phosphorylation regulates not only Nlp oligomerization but also its association with the centrosome. Intriguingly, γ-tubulin was present not only in the large assembly in the presence of kinase-inactive Nek2A, but also in the smaller Nlp fragments that had been displaced from the centrosome by active Nek2A (Fig. 8B). This was not true of other unrelated centrosomal proteins (data not shown). Based on this result, we predicted that the ability of the centrosome to organize a radial array of microtubules would be compromised. Microtubule regrowth assays confirmed that cells containing Nek2A-induced GFP-Nlp fragments failed to produce radial microtubule asters, in contrast to surrounding untransfected cells (Fig. 8C and D). Thus, Nek2A stimulates release of Nlp from the centrosomes but not release of γ-tubulin from Nlp. Furthermore, this indicates that association with the centrosome and the γ-tubulin ring complex are independent properties of the Nlp protein.

Phosphorylation of Nlp by Nek2 in vitro regulates Plk1 phosphorylation. To show that Nek2 is capable of phosphorylating Nlp, in vitro kinase assays were first carried out with the MBP-X-Nlp$_{262–552}$ fusion protein. Active but not inactive

X-Nek2A expressed in insect cells (51) strongly phosphorylated this protein but not MBP alone (Fig. 9A). This fragment was similarly phosphorylated by the *Xenopus* Nek2B kinase and by *Xenopus* Plx1 (data not shown). The N-terminal half of human Nlp containing the eight putative Plk1 phosphorylation sites (GST-Nlp N-term) (3) was also strongly phosphorylated by active but not inactive human Nek2A immunoprecipitated from transfected cells (Fig. 9B and C). Mutation of the eight Plk1 phosphorylation sites significantly reduced phosphorylation by Plk1 but not Nek2A, confirming that the sites phosphorylated by Plk1 and Nek2 are distinct (Fig. 9C and D).

To determine whether phosphorylation of Nlp by Plk1 is regulated by Nek2, we performed Plk1 in vitro kinase assays with the GST-Nlp fragment that had been incubated with either wild-type or kinase-inactive Nek2A in the presence of unlabeled ATP. Strikingly, Nlp that had been incubated with immunoprecipitated active Nek2A was more efficiently phosphorylated than Nlp incubated with kinase-inactive Nek2A (Fig. 9E) or beads alone (Fig. 9F). Taken together, these data support a model in which Nek2A and Plk1 coordinately regulate the association of Nlp with the mother centriole and γ-tubulin ring complex at the G$_2$/M transition and in which Nek2A might act as a priming kinase for Plk1.

DISCUSSION

Centrosomes play a dominant role in generating both the long, relatively stable microtubules present in interphase cells and the highly dynamic microtubule asters present during mitosis (24). For this reason, centrosome abnormalities could contribute to the cell polarity defects and chromosome instability that typify many cancer cells (42). Yet the mechanistic basis by which microtubule asters are organized at centrosomes and spindle poles remains poorly understood, and still less is known about how these are regulated at the G$_2$/M transition. Important progress in this direction came with the identification of a novel centrosomal protein, Nlp, which binds the γ-tubulin ring complex and is a substrate of the mitotic Plk1 kinase. Through characterization of both *Xenopus* and human Nlps, we show here that Nlp is a component of the mother centriole. Furthermore, we demonstrate that Nlp is specifically displaced from centrosomes upon mitotic entry rather than being degraded. Most importantly, we present evidence that Nlp can be phosphorylated not only by Plk1 but also by a second centrosomal kinase, Nek2. We propose that the coordinate regulation of Nlp by Plk1 and Nek2 triggers loss

---

FIG. 4. Nek2A interacts with Nlp and displaces it from the centrosome. (A) Yeast two-hybrid interaction assay. The table on the left indicates the Gal4 DNA-binding domain (DBD) and activation domain (AD) fusion proteins expressed in *S. cerevisiae* with a photograph of the appropriate colonies after 5 days of growth on plates lacking histidine and adenine. The histogram on the right indicates β-galactosidase activity (arbitrary units) of the yeast strains as measured with an *o*-nitrophenylgalactopyranoside assay. Experiments were repeated three times, and error bars show the standard deviation. The activity of the positive control interaction between SNF1 and SNF4 was set at 1.0. (B) *Xenopus* A6 cells were transiently transfected with either human wild-type Myc-Nek2A (a to c) or the Myc-Nek2A-K/R kinase-inactive mutant (d to f) and, after 24 h, methanol fixed and processed for immunofluorescence microscopy with anti-Nek2 (R81, red) and anti-X-Nlp (R1679, green) antibodies. (C) The percentage of A6 cells in which the intensity of X-Nlp at the centrosome was significantly reduced or undetectable was calculated in untransfected cells and cells transfected with wild-type Nek2A or kinase-inactive Nek2A by counting >100 cells in three independent experiments. (D) Human U2OS cells were either untransfected (a to c) or transfected for 24 h with human Myc-Nek2A (d to f) or Myc-Nek2A-K/R (g to i) and stained with antibodies against human Nek2 (red) and Nlp (green). (E) Similarly, U2OS cells were transfected for 24 h with wild-type EGFP-Aurora A (a and b; green) or kinase-inactive EGFP-Aurora A-K162R (c and d; green) before processing with antibodies against endogenous Nlp (red). Scale bars in panels B, D, and E, 10 μm.
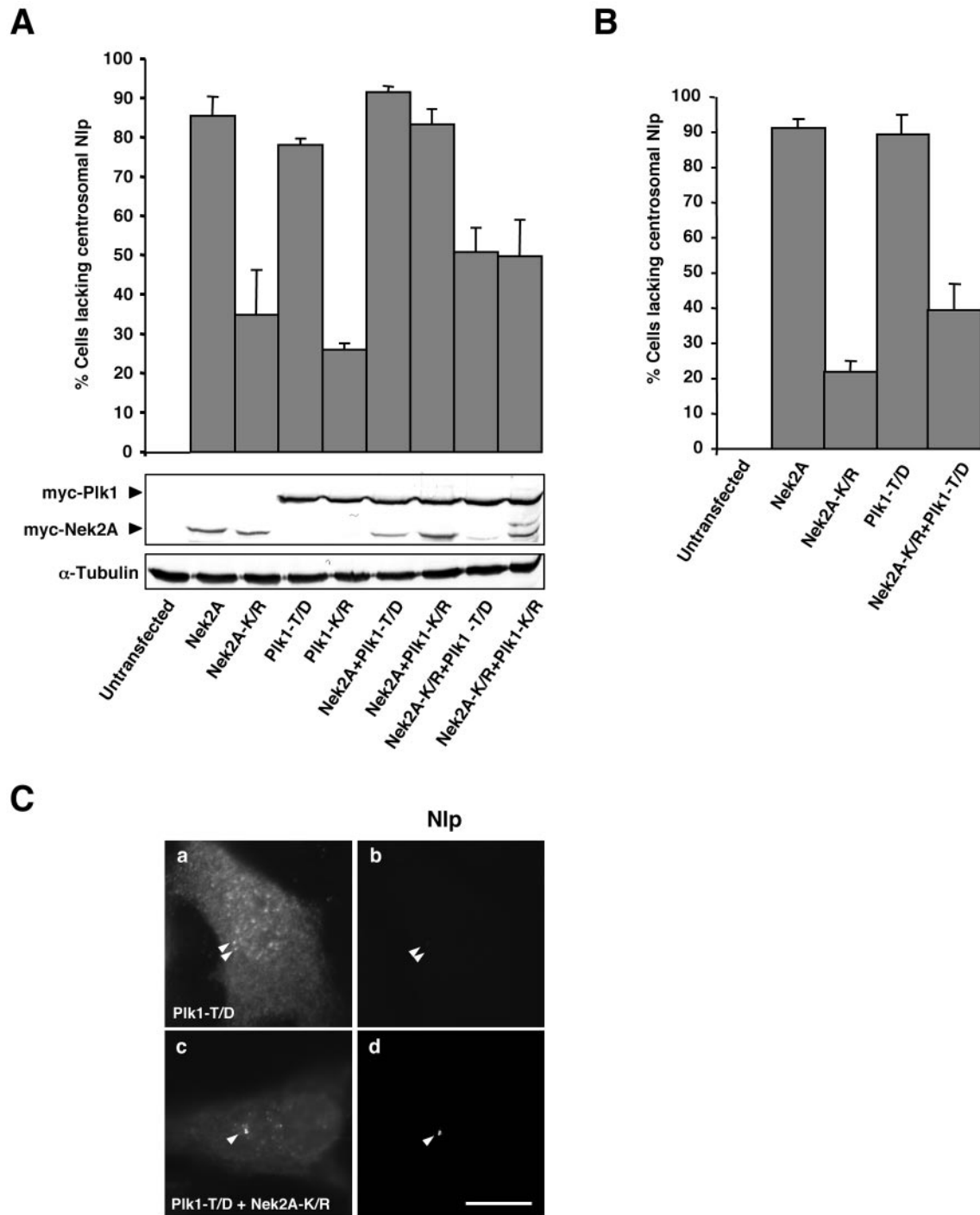
FIG. 5. Displacement of centrosomal Nlp by Plk1 is blocked by kinase-inactive Nek2A. (A) Human U2OS cells were cotransfected for 24 h with Myc-tagged Nek2A, Nek2A-K37R (K/R), Plk1-T210D (T/D), or Plk1-K82R (K/R), as indicated, before methanol fixation and processing by immunofluorescence microscopy with appropriate antibodies to detect transfected proteins (α-Myc) and endogenous Nlp. The percentage of cells with reduced or absent Nlp at interphase centrosomes was calculated in >100 cells for each sample in three independent experiments. Western blots show the level of expression of the transfected proteins (Myc), and equal loading was confirmed with an antitubulin blot. (B) Transient transfections were performed and analyzed as in A except that after only 16 h of transfection. (C) Representative images of endogenous Nlp (b and d) in cells transfected with Plk1-T/D alone (a and b) or in combination with Nek2A-K/R (c and d) are shown. Scale bar, 10 μm.

of interaction of Nlp with both the γ-tubulin ring complex and mother centriole as cells enter mitosis.

Role for Nlp in microtubule anchoring? Microtubules are nucleated from γ-tubulin ring complexes that are evenly dis-

tributed within the pericentriolar material (27). Indeed, microtubule regrowth assays demonstrate that the pericentriolar material associated with mother and daughter centrioles has a similar capacity for microtubule nucleation even when well
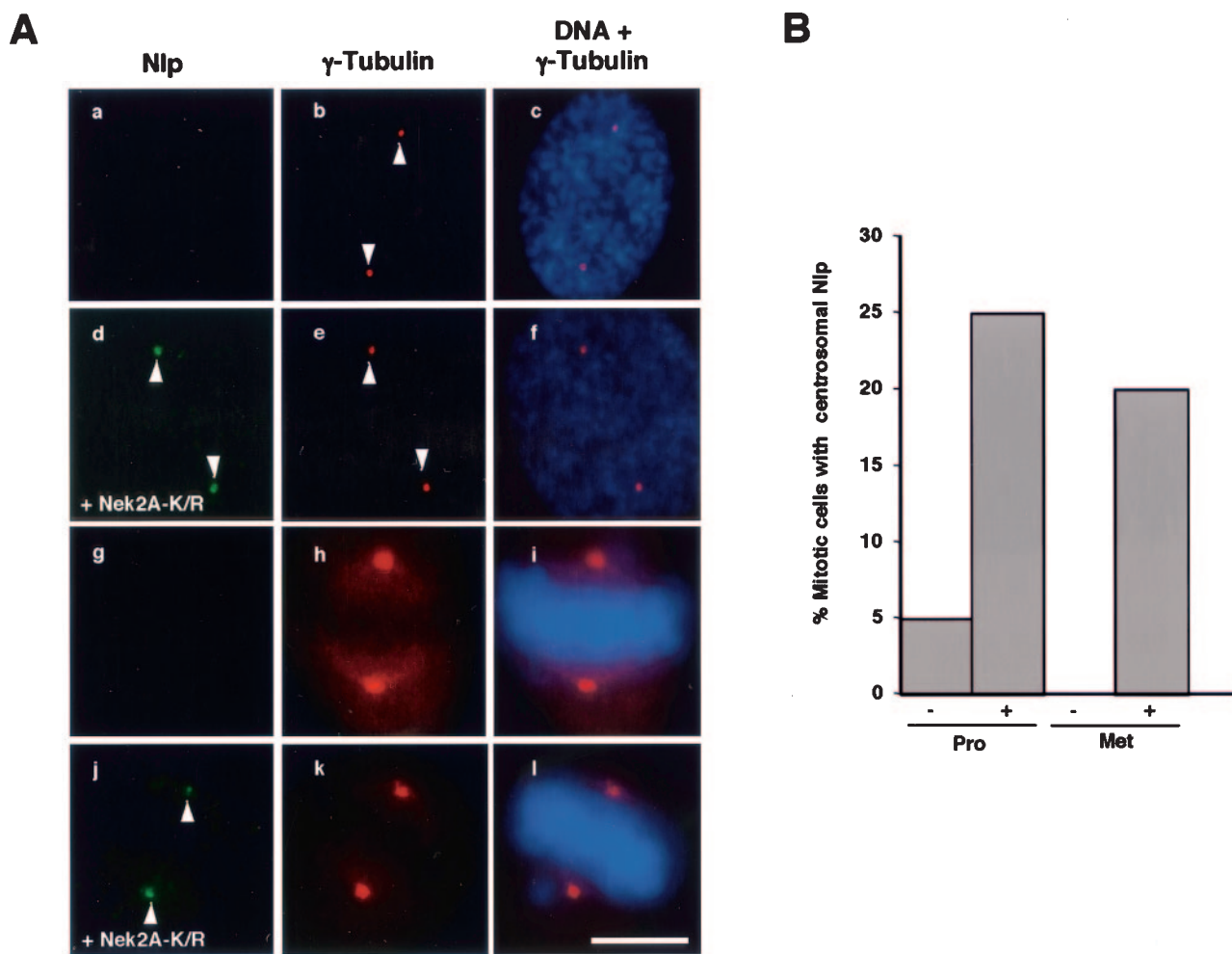
FIG. 6. Kinase-inactive Nek2 interferes with Nlp displacement from mitotic spindle poles. (A) U2OS:Nek2A-K37R-Myc-His cells were either uninduced (a to c and g to i) or induced with tetracycline for 24 h (d to f and j to l) before methanol fixation and processing for immunofluorescence microscopy with antibodies against γ-tubulin (red) or Nlp (green). Merged images of γ-tubulin stain (red) and DNA stained with Hoechst 33258 (blue) are also shown. a to f, prophase cells; g to l, metaphase cells. Scale bar, 5 μm. (B) The percentages of prophase (Pro) and metaphase (Met) cells in which Nlp was readily detected at the spindle poles were calculated in uninduced (−) and induced (+) cells; 40 cells were analyzed for each condition.

separated (38, 44). However, at steady state, most centrosomal microtubules in interphase are associated with the mother centriole, leading to the hypothesis that mother centrioles are associated with microtubule-anchoring activity (1). Our observation that Nlp is a mother centriole-specific protein in *Xenopus* A6 cells supports the hypothesis that it is a microtubule-anchoring protein. Other candidates in vertebrate cells that are mother centriole specific include the related protein ninein as well as dynactin and the small GTPase Ran. Ninein is localized specifically on the subdistal appendages of the mother centriole, and these structures have been proposed as sites of microtubule anchoring (44). Furthermore, ninein is present at noncentrosomal sites of microtubule anchoring in the apical region of cochlear epithelial cells (39). Dynactin is implicated independently of cytoplasmic dynein in interphase microtubule anchoring, as overexpression of dynactin subunits leads to loss of a radially organized centrosomal array of microtubules (45). Ran is also present on mother centriolar appendages, micro-

tubule minus ends, and apical sites of microtubule anchoring, although whether it contributes to microtubule anchoring is unclear (32).

How might Nlp anchor microtubules? During interphase, microtubule minus ends are relatively stable consistent with the idea that they are capped by the γ-tubulin ring complex (30, 40, 53). Hence, microtubule anchoring could occur through direct binding of Nlp to γ-tubulin ring complex components. Indeed, Casenghi and colleagues demonstrated interaction between Nlp and two of the γ-tubulin ring complex components, γ-tubulin and human GCP4 (3). If Nlp anchors microtubules via γ-tubulin ring complex caps, this raises the important question of what regulates the release of γ-tubulin ring complexes from the γ-tubulin binding proteins present throughout the pericentriolar material. One possibility is that microtubule elongation alters the conformation of the γ-tubulin ring complex at its minus end, promoting release from the pericentriolar material-distributed γ-tubulin binding protein.
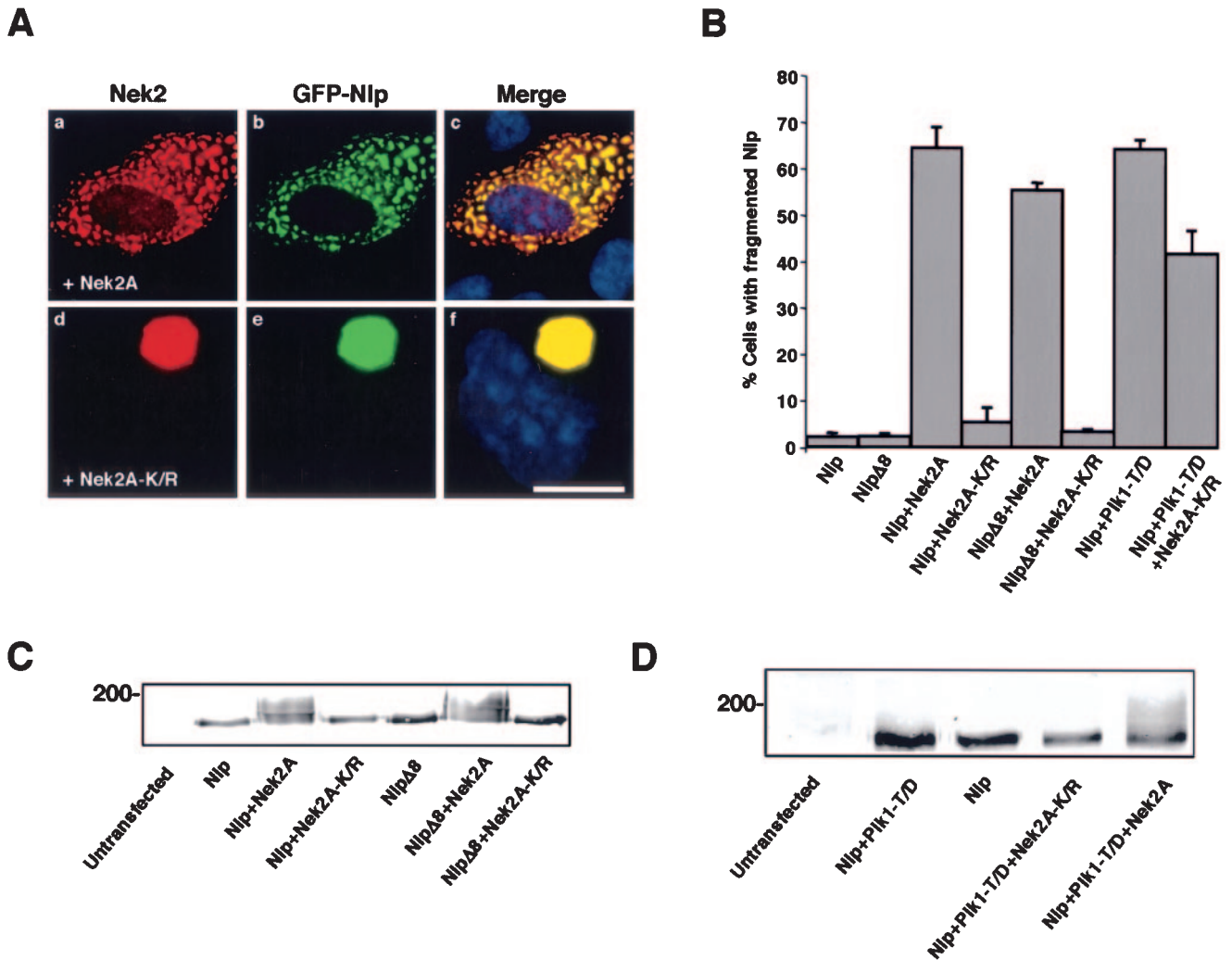
A

B

C

D

FIG. 7. Nek2 displaces GFP-Nlp assemblies from the centrosome. (A) U2OS cells were cotransfected with GFP-Nlp and either wild-type Myc-Nek2A (a to c) or Myc-Nek2A-K/R (d to f) before methanol fixation after 24 h and processing for immunofluorescence microscopy. Anti-Nek2 antibodies (red), GFP signals (green), and merged images including DNA stained with Hoechst 33258 (blue) are shown. Scale bar, 10 μm. (B) The percentage of cells in which recombinant Nlp is fragmented (as opposed to a single large assembly) is presented for each set of cotransfections as indicated; 100 cells were counted for each set, and independent experiments were performed three times. (C) Extracts were prepared from U2OS cells transfected with the Nek2A and GFP-Nlp constructs as indicated and Western blotted with anti-GFP antibodies. An electrophoretic gel mobility shift indicative of phosphorylation was detected in the GFP-Nlp and GFP-NlpΔ8 proteins only in the presence of wild-type Nek2A. (D) An electrophoretic mobility shift of GFP-Nlp induced by Plk1-T/D is lost upon cotransfection with Nek2A-K/R. HeLa cells were transfected as indicated and processed as in panel C.

Alternatively, Nlp may be capable of interacting directly with the minus ends of microtubules, allowing it to anchor microtubules that have been released from nucleation complexes or severed by proteins such as katanin (23). At acentrosomal sites of microtubule anchoring, such as the apical regions of cochlear epithelial cells, γ-tubulin is not present, indicating that microtubule attachment here cannot be via γ-tubulin ring complexes (39). To confirm a role in microtubule anchoring for Nlp, it will be important to examine its precise centriolar localization by immunoelectron microscopy as well as to determine whether, like ninein, it is also present at acentrosomal sites of microtubule anchoring in differentiated cells.

Regulation of Nlp localization through the cell cycle. Previous data suggested that Nlp is present on interphase centrosomes but absent from mitotic spindle poles (3). However, this study had not been able to distinguish whether this was a result of protein degradation or displacement from the centrosome. The generation of antibodies against *Xenopus* Nlp allowed us to quantitate the change in both centrosomal and total cellular abundance of Nlp through the cell cycle. Our results indicated a 10-fold decrease in Nlp association with metaphase spindle poles compared to interphase centrosomes. However, we found no overall change in abundance of total Nlp between interphase and mitotic cells. While localized degradation of
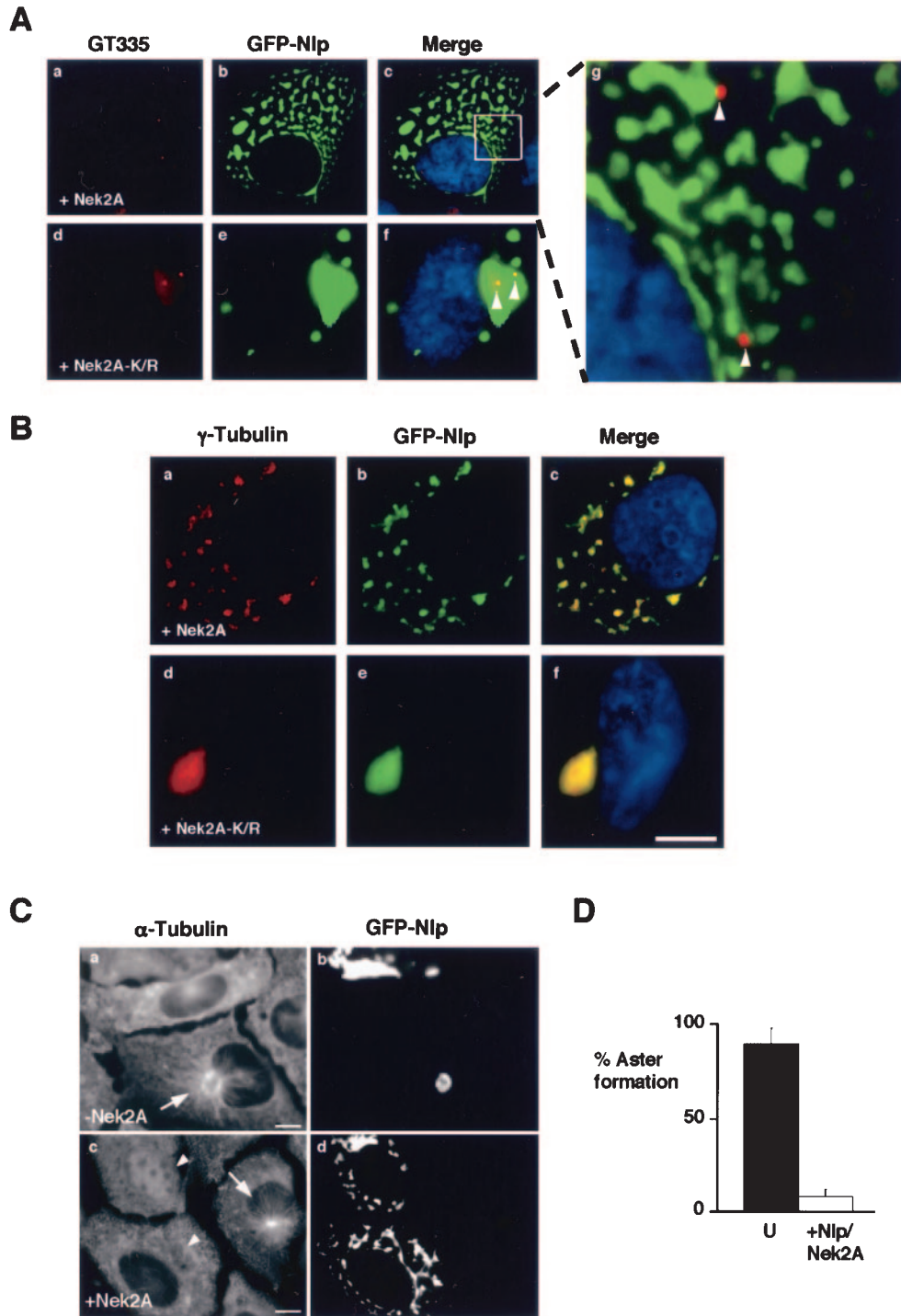
FIG. 8. Nek2 does not prevent association of Nlp with γ-tubulin. (A) U2OS cells were cotransfected with GFP-Nlp and either wild-type Myc-Nek2A (a to c) or Myc-Nek2A-K/R (d to f) before methanol fixation after 24 h and processing for immunofluorescence microscopy. Centrioles stained with GT335 (red), GFP signals (green), and merged images including DNA stained with Hoechst 33258 (blue) are shown. Magnification of the inset box in panel c (g) highlights the fact that GFP-Nlp fragments do not colocalize with centrioles (arrows), whereas centrioles do colocalize with the large GFP-Nlp assembly when coexpressed with kinase-inactive Nek2 (arrows, panel f). (B) Cells processed as for panel A were stained with anti-γ-tubulin antibodies (red). GFP signals (green) and merged images including DNA stained with Hoechst 33258 (blue) are shown. (C) Microtubule regrowth assays were performed on cells transfected with GFP-Nlp alone (a and b) or GFP-Nlp plus Nek2A (c and d). Untransfected cells contain small radial microtubule asters emanating from the centrosome (c, arrow). Cells transfected with GFP-Nlp alone have large microtubule asters surrounding the single GFP-Nlp assembly (a, arrow). However, cells containing fragmented GFP-Nlp lack any such aster (c, arrowheads). (D) Histogram indicating the percentage of untransfected cells (U) with microtubule asters compared to cells cotransfected with GFP-Nlp and Nek2A. Scale bars, 10 μm.
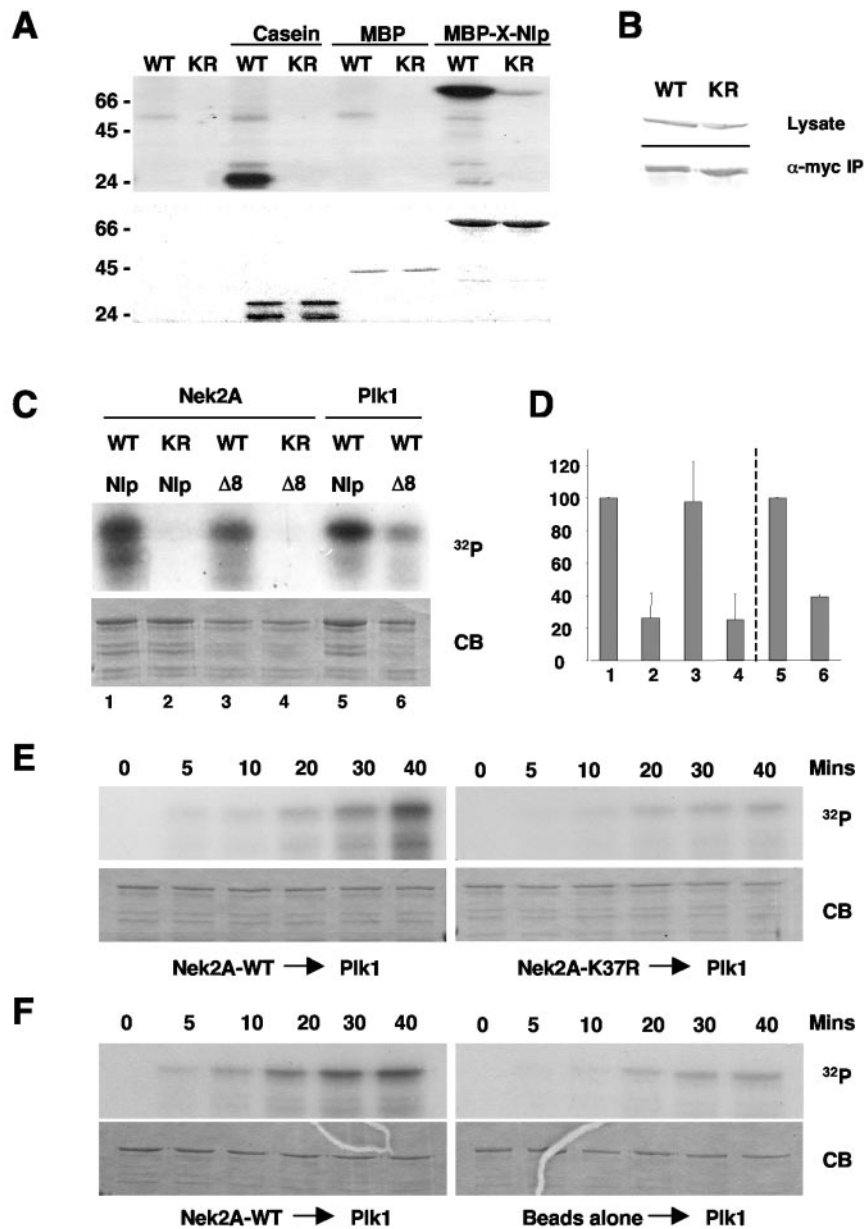
FIG. 9. In vitro phosphorylation of Nlp by Nek2 and Plk1. (A) Purified MBP-X-Nlp$_{262-552}$, MBP alone, and casein were phosphorylated in vitro by wild-type (WT) or kinase-inactive (KR) human Nek2A expressed in insect cells. Samples were separated by SDS-PAGE, stained with Coomassie blue (bottom panel), and exposed to autoradiography (top panel). (B) Western blots indicating equal expression (anti-Myc, top panel) and immunoprecipitation (anti-Nek2, bottom panel) of wild-type and kinase-inactive Myc-Nek2A proteins from transfected HeLa cells for use in kinase assays. (C) GST-Nlp-N-term (Nlp) or GST-Nlp-N-term-Δ8 (Δ8) was phosphorylated in vitro with Nek2A kinases immunoprecipitated from transfected HeLa cells or purified Plk1 expressed in insect cells, as indicated. (D) ^{32}P incorporation into the Nlp proteins as shown in panel C was determined by scintillation counting. The level of phosphorylation of the GST-Nlp-N-term protein by wild-type Nek2 (1–4) and Plk1 (5, 6) was set as 100%. The histogram presents the average of three independent experiments. (E). GST-Nlp-N-term was incubated with either wild-type (left panels) or kinase-inactive (right panels) immunoprecipitated Nek2A for 40 min in the presence of unlabeled ATP. Purified Plk1 was then added together with [γ-^{32}P]ATP and samples were taken at the times indicated before separation by SDS-PAGE. Gels were stained with Coomassie blue (CB) and exposed to autoradiography (^{32}P). In each of five independent experiments, the phosphorylation of Nlp by Plk1 was always greater after incubation with wild-type compared to kinase-inactive Nek2A. (F) Kinase assays were performed as in panel E except that phosphorylation of Nlp by Plk1 was assayed after incubation with either immunoprecipitated Nek2A (left panels) or protein G-Sepharose beads alone (right panels).

Nlp at the centrosome remains a theoretical possibility, our results strongly support a change in localization as being the main cause of loss of Nlp staining at mitotic spindle poles. In this respect, Nlp localization is regulated very similarly to an-

other centriolar protein, C-Nap1, which is also a substrate of Nek2 (16, 34). Interestingly, Nlp was not present in cytoplasmic extracts of either mitotic or interphase eggs, nor was it detected on the basal bodies of sperm either before or after

incubation in egg extract. Thus, it appears that Nlp is not a core component of basal bodies, nor is it required for microtubule organization during early embryonic development.

Nlp is a novel substrate of the Nek2 kinase. The specific displacement of Nlp from the centrosome at the G_2/M transition makes it a likely target for regulation by cell cycle-dependent phosphorylation. Indeed, there is good evidence that Nlp is a target for the Plk1 kinase and that Plk1 activity can regulate its association with the centrosome (3). However, recent studies have revealed that recognition of certain substrates by Plk1 is promoted by prior phosphorylation by other kinases (11), and here we show that Nlp is also a target for the Nek2 centrosomal kinase. Nlp can interact with and be phosphorylated by Nek2 both in vitro and in vivo. Meanwhile, overexpression of active Nek2, like Plk1, displaces both endogenous and recombinant Nlp from the interphase centrosome. The fact that Nek2 can equally phosphorylate and displace the Nlp mutant lacking Plk1 phosphorylation sites demonstrates that Nek2 is targeting different sites to Plk1.

Intriguingly, while Nek2 perturbs the association of Nlp with the centrosome, it does not appear to interfere with the interaction of Nlp with γ-tubulin. As a result, cells with fragmented Nlp assemblies fail to nucleate radial microtubule asters because the bulk of the γ-tubulin ring complexes is associated with noncentrosomal recombinant Nlp. Previously, we reported that overexpressing Nek2 alone also leads to loss of γ-tubulin from the centrosome and failure to organize radial microtubule arrays (17). At the time, we interpreted this as a result of dispersal of centrosome structure, but our current study highlights the possibility that this is the direct result of displacement of endogenous Nlp. Certainly, our results on the effect of Nek2 overexpression on microtubule organization are consistent whether Nlp is coexpressed or not.

Coordinate regulation of Nlp by Nek2 and Plk1. Recognition of mitotic substrates by polo-like kinases is promoted by direct interaction between the substrate and polo box motifs in the C-terminal noncatalytic domain of the kinase (46). Plk1 contains two highly conserved polo boxes that together comprise a polo box domain that is important for subcellular localization and autoinhibition. Structural studies have revealed that each polo box motif forms a single six-stranded β-sheet, which come together in the polo box domain to form a 12-stranded beta sandwich (4, 10). This acts as a novel recognition motif for phosphorylated peptides, which sit in the middle of the sandwich.

Degenerate-peptide library screening revealed that the optimal target site for the polo box domain was S-p(S/T) (11). Thus, tight interaction of Plk1 with its substrates is stimulated by their prior phosphorylation on serine or threonine in this consensus. Both Cdk1 and Plk1 have been proposed as priming kinases for Plk1 (11, 41), with two of the putative Plk1 sites identified in Nlp being within a polo box domain recognition consensus (S88 and T161). Our data, however, raise the possibility that Nek2 is a third priming kinase for Plk1. First, kinase-dead Nek2A interfered with the ability of Plk1 to displace Nlp from the large aggregates around the centrosome but not vice versa, putting Nek2 upstream of Plk1 in the regulation of Nlp. Second, expression of kinase-dead Nek2A led to a significant increase in the amount of endogenous Nlp present on mitotic spindle poles. Third, incubation of Nlp with

Nek2 in vitro stimulated the level of Nlp phosphorylation by Plk1. This study therefore not only describes the first example of a centrosomal substrate phosphorylated by both the Plk1 and Nek2 kinases in vitro, but also supports the hypothesis that phosphorylation of Nlp by Nek2 promotes its phosphorylation by Plk1. Importantly, studies in fission yeast also support a role for NIMA-related kinases in promoting recruitment of polo kinases to the spindle pole body (SPB), the fungal equivalent of the centrosome (20). Overexpression of Fin1, the closest relative of Nek2 in *S. pombe*, leads to premature recruitment of the polo kinase Plo1 to the SPB. There is no evidence that Plo1 can be phosphorylated by Fin1, leaving open the possibility that Fin1 is phosphorylating SPB components, thereby facilitating the binding of Plo1. The goal now is to identify sites in Nlp that are phosphorylated by the Nek2 kinase and determine whether their phosphorylation is required for recruitment of Plk1.

REFERENCES

1. **Bornens, M.** 2002. Centrosome composition and microtubule anchoring mechanisms. Curr. Opin. Cell Biol. **14:**25–34.
2. **Bouckson-Castaing, V., M. Moudjou, D. J. Ferguson, S. Mucklow, Y. Belkaid, G. Milon, and P. J. Crocker.** 1996. Molecular characterization of ninein, a new coiled-coil protein of the centrosome. J. Cell Sci. **109:**179–190.
3. **Casenghi, M., P. Meraldi, U. Weinhart, P. I. Duncan, R. Korner, and E. A. Nigg.** 2003. Polo-like kinase 1 regulates Nlp, a centrosome protein involved in microtubule nucleation. Dev. Cell **5:**113–125.
4. **Cheng, K.-Y., E. D. Lowe, J. Sinclair, E. A. Nigg, and L. N. Johnson.** 2003. The crystal structure of the human polo-like kinase-1 polo box domain and its phospho-peptide complex. EMBO J. **22:**5757–5768.
5. **Compton, D. A.** 2000. Spindle assembly in animal cells. Annu. Rev. Biochem. **69:**95–114.
6. **Dictenberg, J. B., W. Zimmerman, C. A. Sparks, A. Young, C. Vidair, Y. Zheng, W. Carrington, F. S. Fay, and S. J. Doxsey.** 1998. Pericentrin and g-tubulin form a protein complex and are organized into a novel lattice at the centrosome. J. Cell Biol. **141:**163–174.
7. **do Carmo Avides, M., and D. M. Glover.** 1999. Abnormal spindle protein, Asp, and the integrity of mitotic centrosomal microtubule organizing centers. Science **283:**1733–1735.
8. **Doxsey, S.** 2001. Re-evaluating centrosome function. Nat. Revs: Mol. Cell. Biol. **2:**688–698.
9. **Durfee, T., K. Becherer, P.-L. Chen, S.-H. Yeh, Y. Yang, A. E. Kilburn, W.-H. Lee, and S. J. Elledge.** 1993. The retinoblastoma protein associates with the protein phosphatase type 1 catalytic subunit. Genes Dev. **7:**555–569.
10. **Elia, A. E., P. Rellos, L. F. Haire, J. W. Chao, F. J. Ivins, K. Hoepker, D. Mohammad, L. C. Cantley, S. J. Smerdon, and M. B. Yaffe.** 2003b. The molecular basis for phosphodependent substrate targeting and regulation of Plks by the Polo-box domain. Cell **115:**83–95.
11. **Elia, A. E. H., L. C. Cantley, and M. B. Yaffe.** 2003a. Proteomic screen finds pSer/pThr-binding domain localizing Plk1 to mitotic substrates. Science **299:**1228–1231.
12. **Faragher, A. J., and A. M. Fry.** 2003. Nek2 kinase stimulates centrosome disjunction and is required for formation of bipolar mitotic spindles. Mol. Biol. Cell **14:**2876–2889.
13. **Fry, A. M.** 2002. The Nek2 protein kinase: a novel regulator of centrosome structure. Oncogene **21:**6184–6194.
14. **Fry, A. M., L. Arnaud, and E. A. Nigg.** 1999. Activity of the human centrosomal kinase, Nek2, depends upon an unusual leucine zipper dimerization motif. J. Biol. Chem. **274:**16304–16310.
15. **Fry, A. M., P. Descombes, C. Twomey, R. Bacchieri, and E. A. Nigg.** 2000.

The NIMA-related kinase X-Nek2B is required for efficient assembly of the zygotic centrosome in *Xenopus laevis.* J. Cell Sci. **113:**1973–1984.

16. **Fry, A. M., T. Mayor, P. Meraldi, Y.-D. Stierhof, K. Tanaka, and E. A. Nigg.** 1998b. C-Nap1, a novel centrosomal coiled-coil protein and candidate substrate of the cell cycle-regulated protein kinase Nek2. J. Cell Biol. **141:**1563–1574.

17. **Fry, A. M., P. Meraldi, and E. A. Nigg.** 1998a. A centrosomal function for the human Nek2 protein kinase, a member of the NIMA-family of cell cycle regulators. EMBO J. **17:**470–481.

18. **Fry, A. M., and E. A. Nigg.** 1997. Characterization of mammalian NIMA-related kinases. Methods Enzymol. **283:**270–282.

19. **Golsteyn, R. M., K. E. Mundt, A. M. Fry, and E. A. Nigg.** 1995. Cell cycle regulation of the activity and subcellular localization of PLK1, a human protein kinase implicated in mitotic spindle function. J. Cell Biol. **129:**1617–1628.

20. **Grallert, A., and I. M. Hagan.** 2002. *S. pombe* NIMA related kinase, Fin1, regulates spindle formation, and an affinity of Polo for the SPB. EMBO J. **21:**3096–3107.

21. **Hames, R. S., and A. M. Fry.** 2002. Alternative splice variants of the human centrosomal kinase Nek2 exhibit distinct patterns of expression in mitosis. Biochem. J. **361:**77–85.

22. **Hames, R. S., S. L. Wattam, H. Yamano, R. Bacchieri, and A. M. Fry.** 2001. APC/C-mediated destruction of the centrosomal kinase Nek2A occurs in early mitosis and depends upon a cyclin A-type D-box. EMBO J. **20:**7117–7127.

23. **Hartman, J. J., J. Mahr, K. McNally, K. Okawa, A. Iwamatsu, S. Thomas, S. Cheesman, J. Heuser, R. D. Vale, and F. J. McNally.** 1998. Katanin, a microtubule-severing protein is a novel AAA ATPase that targets to the centrosome using a WD40-containing subunit. Cell **93:**277–287.

24. **Heald, R., R. Tournebize, A. Habermann, E. Karsenti, and A. Hyman.** 1997. Spindle assembly in Xenopus egg extracts: respective roles of centrosomes and microtubule self-organization. J. Cell Biol. **138:**615–628.

25. **James, P., J. Halladay, and E. A. Craig.** 1996. Genomic libraries and a host strain designed for highly efficient two-hybrid selection in yeast. Genetics **144:**1425–1436.

26. **Jang, Y., C. Lin, S. Ma, and R. L. Erikson.** 2002. Functional studies on the role of the C-terminal domain of mammalian polo-like kinase. Proc. Natl. Acad. Sci. USA **99:**1984–1989.

27. **Job, D., O. Valiron, and B. Oakley.** 2003. Microtubule nucleation. Curr. Opin. Cell Biol. **15:**111–117.

28. **Kawaguchi, S., and Y. Zheng.** 2004. Characterization of a Drosophila centrosome protein CP309 that shares homology with kendrin and CG-NAP. Mol. Biol. Cell **15:**37–45.

29. **Keating, T. J., and G. G. Borisy.** 1999. Centrosomal and non-centrosomal microtubules. Biol. Cell **91:**321–329.

30. **Keating, T. J., and G. G. Borisy.** 2000. Immunostructural evidence for the template mechanism of microtubule nucleation. Nat. Cell Biol. **2:**352–357.

31. **Kelm, O., M. Wind, W. D. Lehmann, and E. A. Nigg.** 2002. Cell cycle-regulated phosphorylation of the *Xenopus* polo-like kinase Plx1. J. Biol. Chem. **277:**25247–25256.

32. **Keryer, G., B. Di Fiore, C. Celati, K. F. Lechtreck, M. Mogensen, A. Delouvee, P. Lavia, M. Bornens, and A.-M. Tassin.** 2003. Part of Ran is associated with AKAP450 at the centrosome: involvement in microtubule-organizing activity. Mol. Biol. Cell **14:**4260–4271.

33. **Lupas, A.** 1996. Prediction and analysis of coiled-coil structures. Methods Enzymol. **266:**513–525.

34. **Mayor, T., U. Hacker, Y.-D. Stierhof, and E. A. Nigg.** 2002. The mechanism

regulating dissociation of the centrosomal protein C-Nap1 from mitotic spindle poles. J. Cell Sci. **115:**3275–3284.

35. **Mayor, T., K. Tanaka, Y.-D. Stierhof, A. M. Fry, and E. A. Nigg.** 2000. The centrosomal protein C-Nap1 displays properties supporting a role in cell cycle-regulated centrosome cohesion. J. Cell Biol. **151:**837–846.

36. **McIntosh, J. R., E. L. Grishchuk, and R. R. West.** 2002. Chromosome-microtubule interactions during mitosis. Annu. Rev. Cell Dev. Biol. **18:**193–219.

37. **Meraldi, P., R. Honda, and E. A. Nigg.** 2002. Aurora-A overexpression reveals tetraploidization as a major route to centrosome amplification in p53$^{-/-}$ cells. EMBO J. **21:**483–492.

38. **Meraldi, P., and E. A. Nigg.** 2001. Centrosome cohesion is regulated by a balance of kinase and phosphatase activities. J. Cell Sci. **114:**3749–3757.

39. **Mogensen, M. M., A. Malik, M. Piel, V. Bouckson-Castaing, and M. Bornens.** 2000. Microtubule minus-end anchorage at centrosomal and non-centrosomal sites: the role of ninein. J. Cell Sci. **113:**3013–3023.

40. **Moritz, M., M. B. Braunfeld, V. Guenebaut, J. Heuser, and D. A. Agard.** 2000. Structure of the g-tubulin ring complex: a template for microtubule nucleation. Nat. Cell Biol. **2:**365–370.

41. **Neef, R., C. Preisinger, J. Sutcliffe, R. Kopajtich, E. A. Nigg, T. U. Mayer, and F. A. Barr.** 2003. Phosphorylation of mitotic kinesin-like protein 2 by polo-like kinase 1 is required for cytokinesis. J. Cell Biol. **162:**863–875.

42. **Nigg, E. A.** 2002. Centrosome aberrations: cause or consequence of cancer progression? Nat. Rev. Cancer **2:**815–825.

43. **Nigg, E. A.** 2001. Mitotic kinases as regulators of cell division and its checkpoints. Nat. Rev. Mol. Cell. Biol. **2:**21–32.

44. **Piel, M., P. Meyer, A. Khodjakov, C. L. Rieder, and M. Bornens.** 2000. The respective contributions of the mother and daughter centrioles to centrosome activity and behaviour in vertebrate cells. J. Cell Biol. **149:**317–329.

45. **Quintyne, N. J., S. R. Gill, D. M. Eckley, C. L. Crego, D. A. Compton, and T. A. Schroer.** 1999. Dynactin is required for microtubule anchoring at fibroblast centrosomes. J. Cell Biol. **147:**321–334.

46. **Reynolds, N., and H. Ohkura.** 2003. Polo boxes form a single functional domain that mediates interactions with multiple proteins in fission yeast polo kinase. J. Cell Sci. **116:**1377–1387.

47. **Schroer, T. A.** 2001. Microtubules don and doff their caps: dynamic attachments at plus and minus ends. Curr. Opin. Cell Biol. **13:**92–96.

48. **Seong, Y.-S., K. Kamijo, J.-S. Lee, E. Fernandez, R. Kuriyama, T. Miki, and K. S. Lee.** 2002. A spindle checkpoint arrest and a cytokinesis failure by the dominant-negative polo-box domain of Plk1 in U-2 OS cells. J. Biol. Chem. **277:**32282–32293.

49. **Song, S., T. Z. Grenfell, S. Garfield, R. L. Erikson, and K. S. Lee.** 2000. Essential function of the polo box of Cdc5 in subcellular localization and induction of cytokinetic structures. Mol. Cell. Biol. **20:**286–298.

50. **Takahashi, M., A. Yamagiwa, T. Nishimura, H. Mukai, and Y. Ono.** 2002. Centrosomal proteins CG-NAP and kendrin provide microtubule nucleation sites by anchoring gamma-tubulin ring complex. Mol. Biol. Cell **13:**3235–3245.

51. **Twomey, C., S. L. Wattam, M. R. Pillai, J. Rapley, J. E. Baxter, and A. M. Fry.** 2004. Nek2B stimulates zygotic centrosome assembly in *Xenopus laevis* in a kinase-independent manner. Dev. Biol. **265:**384–398.

52. **Uto, K., N. Nakajo, and N. Sagata.** 1999. Two structural variants of Nek2 kinase, termed Nek2A and Nek2B, are differentially expressed in *Xenopus* tissues and development. Dev. Biol. **208:**456–464.

53. **Wiese, C., and Y. Zhang.** 2000. A new function for the gamma-tubulin ring complex as a microtubule minus-end cap. Nat. Cell Biol. **2:**358–364.